N. Jb. Geol. Paläont. Abh. 261/2, 151–164
published online April 2011

Article

Petrogenesis of Upper Paleozoic post-collisional peraluminous leucogranites, Sierra de Ancasti, northwest Argentina

Alejandro J. Toselli, Juana N. Rossi, Miguel A.S. Basei and Claudia R. Passarelli

With 10 figures and 3 tables

Toselli, A.J., Rossi, J.N., Basei, M.A.S. & Passarelli, C.R. (2011): Petrogenesis of Upper-Paleozoic post-collisional peraluminous leucogranites, Sierra de Ancasti, -northwest Argentina. – N. Jb. Geol. Paläont., Abh., **261**: 151–164; Stuttgart.

Abstract: The Santa Rosa and Sauce Guacho plutons are two post-collisional peraluminous Late Devonian to Early Carboniferous leucogranites that intruded the banded schists of the Ancasti Formation. The leucogranites are composed of microcline phenocrysts along with quartz, plagioclase, muscovite, biotite, ilmenite, tourmaline, apatite, monazite and zircon. Their geochemical composition is consistent with S-type granites and mineralogically they belong to MPG granites (muscovite-peraluminous granites). It is proposed that granite magma generation was related to shear zones that concentrated fluids in the metasedimentary crust during a collision or transcurrent tectonics. U-Pb analyses on monazite gave an age of 369.8 ± 5.3 Ma, while Sm/Nd isotopic data yield $\varepsilon_{Nd(t)}$ values of -5.3 for Sauce Guacho and -5.7 for Santa Rosa indicating crustal provenance. Nd model ages between 1,544 and 1,571 Ma are within the range of magmatic rocks from the Lower Ordovician Famatinian Arc in the Central Sierras Pampeanas.

Key words: Leucogranites, peraluminous, post-collisional, Upper-Paleozoic, Sierras Pampeanas, U-Pb geochronology

Resumen: Los plutones de Santa Rosa y Suace Guacho son granitos peraluminosos post-colisionales del Devónico superior al Carbonífero inferior, que intruyen en los esquistos bandeados de la Formación Ancasti. Ambos son leucogranitos compuestos por fenocristales de microclina, con cuarzo, plagioclasa, moscovita, biotita, ilmenita, turmalina, apatita, monacita y circón. La composición química corresponde a granitos tipo-S y la mineralogía permite su asignación a los granitos MPG (granitos peraluminosos con moscovita). La génesis se relacionaría con fusión en zonas de cizalla que concentran fluidos en la corteza metasedimentaria durante una tectónica de colisión o de transcurrencia. La edad U-Pb sobre monacita es de 369,8 ± 5,3 Ma, y las determinaciones Sm-Nd, dan para Sauce Guacho valores de εNdt de -5,3 y para Santa Rosa εNdt de -5,7, que evidencian proveniencia cortical. Las edades modelo de Nd de 1.544 a 1.571 Ma se corresponden con el rango del Arco Famatiniano de las Sierras Pampeanas Centrales.

Palabras clave: Leucogranitos, peraluminosos, post-colisionales, Paleozoico superior, Sierras Pampeanas, Geocronología U-Pb.

DOI: 10.1127/0077-7749/2011/0152
www.schweizerbart.de
0077-7749/2011/0152 $ 3.50

Introduction

The Carboniferous granites exposed in the Northern Sierras Pampeanas, are represented in general by undeformed plutons that had been intruded passively into Ordovician granitoids or into low-grade metamorphic rocks (Fig. 1). Good examples are the Huaco-Sanagasta, and San Blas-Asha granites which are intrusive in Ordovician granitoides in the Sierra de Velasco (Toselli et al. 2006, 2007; Grosse et al. 2009; Söllner et al. 2007). As these plutons are well-studied some geochronological and geochemical data are available. Other granites of this age but with geochemical and isotopical data not available intruded into low-grade metamorphic rocks. Examples are the Quimivil granite in the Sierra de Zapata (Lazarte et al. 1999); Los Ratones and other minor bodies in the Sierra de Fiambalá (Arrospide 1985; Neugebauer 1995; Grissom et al. 1998; Lazarte et al. 2006), and Papachacra granite in the Sierra de Papachacra (a fluor-rich, topaz-bearing granite, Lazarte et al. 2006) (Fig. 1A).

The basement of the Sierra de Ancasti was intruded by a number of small plutons with different petrographical, geochemical, and geochronological characteristics, from Late Cambrian gabbros, Early Ordovician granites (s. l.) and Late Devonian to Early Carboniferous anatectic leucogranites (Fig. 1B).

The dominant country rocks in the Sierra de Ancasti are composed of banded and poly-deformed medium-grade schists and gneisses, which are regionally known as the Ancasti Formation. Based on Willner (1983) and Reissinger (1983) the tectonic evolution can be characterized by

1) relicts of D1 folding,
2) a NNW-SSE trending (D2) intensive isoclinal folding with formation of the main banding M2 of low-grade regional metamorphism. It is also characterized by local intrusions of Late Cambrian small ultramafic and gabbroid bodies and Lower Ordovician syn-kinematic quartz-diorites and granodiorites,
3) a third deformational event (D3) identifiable by NNW-SSE trending, tight minor folds and large-scale flexures with M3 from the cordierite-staurolite-andalusite zone up to the cordierite-sillimanite-potassium-feldspar zone. The climax of Ordovician magmatic activity is characterized by stock-shaped intrusions of barren two-mica granites reaching a high plutonic level (Reissinger 1983; Toselli et al. 1983, 2002),
4) D4 characterized by local NW-SE trending minor folds presenting a weak schistosity associated with a M4 wide-spread retrograde growth of chlorite and recrystallization of muscovite and quartz,
5) a D5 phase represented by a wide-spread cataclasis which culminates in some narrow mylonitization zones caused by intensive uplift in Devonian ages. This deformative event was followed by the Upper Devonian to Lower Carboniferous post-kinematic intrusion of two-mica "fertile" peraluminous leucogranites, which are enriched in F, B, Li and Be, associated with late wide-spread tourmaline-muscovite pegmatites, spodumen-pegmatites and beryl-pegmatites.

The Lower Carboniferous post-collisional stock granites and leucogranites are subject of this work because they represent the last intrusive magmatic activity in the Sierras Pampeanas and are much less known than the big Ordovician batholiths that dominate the Northern Sierras Pampeanas. Moreover, many of these relatively small plutons are considered fertile, a fact worth to be looked into for a better understanding of their petrogenesis, evolution, emplacement and possible sources of magma generation.

The Santa Rosa (SR) and Sauce Guacho (SG) plutons are the only leucogranites in the north of the Sierra de Ancasti which are related to Be-B-Li pegmatites and fluorite veins.

This paper is part of a comprehensive study conducted in the Sierra de Ancasti on the geology of the Western Pampean Ranges Carboniferous granites, which in comparison with other areas (Eastern Sierras Pampeanas) remains poorly studied. Reported are the main geochemical characteristics of the leucogranites which are compared with other well-known geological areas bearing similar characteristics. Also described is the probable behavior of major and trace elements in these granites, based on recent experimental studies, and its significance for the magmatic evolution as a whole.

Sauce Guacho and Santa Rosa plutons of the Sierra de Ancasti

Field relationships and petrography

The Sauce Guacho (SG) and Santa Rosa (SR) plutons of the Sierra de Ancasti are intrusive into banded schists of the Ancasti Formation showing NNE-SSW-oriented sub-elliptic forms (Fig.1B). Their granites are light reddish- to pink-colored, have very sharp contacts with their wall rocks and do not show evidences of deformation. Locally, miarolitic cavities are present. They are interpreted by Toselli et al. (1983) and Lazarte et al. (2006) as post-tectonic intrusions. Effects of contact metamorphism in the country rocks are not observed. NNE-SSW-trending transtensive

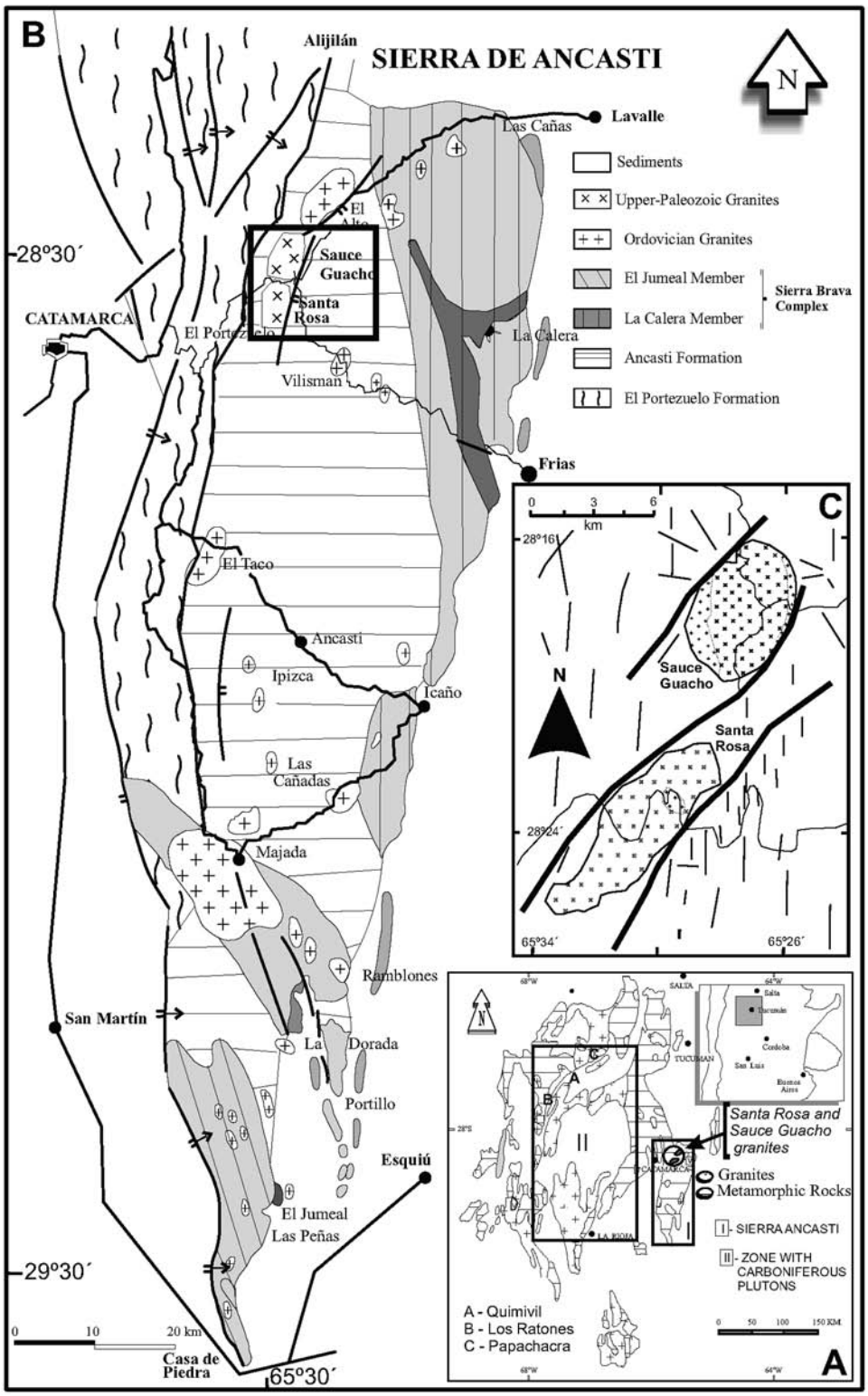

Fig. 1. **A**: Sketch of Sierras Pampeanas with situations of the cited Carboniferous granites. **B**: Simplified geological map of Sierra de Ancasti, with detail of geologic situation of the Sauce Guacho and Santa Rosa plutons. Modified after Aceñolaza et al. (1983). **C**: Simplified geological sketch of Sauce Guacho and Santa Rosa granites of the Sierra de Ancasti.

type faults are present bordering the contacts of both granites. Aplite and pegmatite dikes related to E-W-directed joints cross-cut both plutons.

Typical characteristics of both intrusive bodies are the NE-SW-running fluorite bearing veins associated with a later NE-SW direction of faulting (Reissinger & Miller 1982).

The **Sauce Guacho** granite is an oval-shaped pluton with a NE-SW-length of 6.5 km and a width of 3.7 km. Thin radial fractures are developed outside of the pluton, with the biggest fractures developed in the northwestern part of the surrounding Ancasti Formation schists (Fig. 1C).

The central zone of the SG is a medium- to coarse-grained porphyritic granite. For a width of 300 m, its northern and northeastern rim zone is constituted of fine porphyritic granite conforms. Mineralogically, it is composed of microcline phenocrysts, quartz, plagioclase (An10-14), muscovite and small amounts of biotite (< 5 wt%). K-feldspar shows crossed-twinning, and polysynthetic twinning is well-developed in the plagioclase. The accessory minerals are ilmenite, tourmaline, apatite, monazite and zircon. All the feldspars are affected by sericitization.

The **Santa Rosa** (SR) granite is located 3 km to the SW of the SG granite. It is a pluton with an oval outline with a length of 13.1 km in NE-SW direction and a maximum width of 3.3 km. In parts, the eastern contact is controlled by a NE-SW regional fault (Fig. 1C).

Frequent inclusions of banded-schists of the Ancasti Formation are present in the SR granite. It is composed of mainly porphyritic granite of medium to fine grain size. The mineral composition is similar to that of the SG pluton, but biotite is more frequent than muscovite. K-feldspar shows perthite veins, and the plagioclase (An14-25) has well-developed polysynthetic twinning.

Using K/Ar dating on biotite Linares (1977) assigned an age of 373 ± 10 Ma to the SR granite. For the SG granite the Rb-Sr whole-rock isochron yielded 333.9 ± 10.7 Ma, with an initial ratio of $^{87}Sr/^{86}Sr = 0.715 \pm 0.004$ (Knüver & Miller 1982).

Magnetic susceptibility

Ishihara (1977, 1981) used magnetic susceptibility for discriminating between magnetite- and ilmenite series granitoids. They proposed that the boundary between these two groups be placed at approximately 3.0×10^{-3} SI units.

The magnetic susceptibility was measured in the field using the magnetic susceptibility meter KT-9 Kappameter. In large outcrops of the plutons, field measurements of the magnetic susceptibility at different points vary very little suggesting that superficial alteration has not modified the magnetic susceptibility value of the granites.

In the SG pluton, magnetic susceptibility yielded values between 0.12 and 0.06×10^{-3} SI. A value of 0.25×10^{-3} SI was found the in biotite-granite of the SR pluton, whereas in its muscovite-granite the values varied between 0.10 and 0.06×10^{-3} SI. The magnetic susceptibility data found indicate that both granites are related to ilmenite-series granitoids of Ishihara (1981) and belong to a late- to post-tectonic setting.

Whole rock geochemistry

Major elements

Chemical analyses of whole-rock major, minor and trace elements were carried out at the Actlabs Laboratory (Canada), using a standardized method that is a combination of lithium metaborate/tetraborate fusion with determinations of high precision for INAA and ICP-WRA and ICP/MS, using for external standard calibration of natural and synthetic materials.

The results of the major oxides of the SR and SG granites are presented in Table 1A, those of the trace elements in Table 1B.

The analyzed samples from the SR and SG plutons are variably peraluminous with ACNK (molar Al_2O_3 / [CaO + Na_2O + K_2O]) values between 1.02 and 1.35 and between 1.12 and 1.37 respectively (Fig. 2A).

In the SR pluton, SiO_2 abundance ranges from 70.0 to 76.22% with an average value of 71.75%, Na_2O from 2.03 to 4.99%, K_2O from 1.14 to 8.32%, and the K_2O+Na_2O values range from 3.17 to 13.31% with an average of 8.24%. Fe_2O_3 abundance ranges from 0.76 to 3.07%, MgO from 0.16 to 1.24%, TiO_2 from 0.10 to 0.58%, P_2O_5 from 0.03 to 0.32% Sr abundance ranges from 18 to 158 ppm with an average value of 118.5 ppm.

SiO_2 abundance of the SG pluton ranges from 73.13 to 76.46% averaging 74.54%, Na_2O from 1.69 to 3.42%, K_2O from 4.63 to 5.88%, and the K_2O+Na_2O values range from 6.32 to 9.30% with an average of 7.81%. Fe_2O_{3t} abundance ranges from 0.76 to 1.76% MgO from 0.05 to 0.51%, TiO_2 from 0.09 to 0.26%, and P_2O_5 from 0.11 to 0.30%. Sr abundance ranges from 25 to 78 ppm with an average value of 45 ppm.

The mean contents of K_2O (5.41%), Na_2O (2.81%), and TiO_2+Fe_2O_{3t}+MgO (generally < 2.5%) are charac-

Table 1. **A**. Selected representative major oxide compositions (wt%) of the studied granitic rocks from the Sauce Guacho (SG) and Santa Rosa (SR) plutons. **B:** Selected representative trace element compositions (ppm) of the studied granitic rocks from the Sauce Guacho (SG) and Santa Rosa (SR) plutons.

A	**SAUCE GUACHO GRANITE**										**SANTA ROSA GRANITE**										
Sample	6230	6231	6232	6233	6234	6237	6240	8000	8001	8006	6247	6250	6253	6254	6255	6463b	6467	8002	8003	8007	8027
Rock type	2m	2m	2m	2m	2m	2m	2m	2m	2m	2m	btg	btg	btg	btg	btg	btg	btg	btg	btg	mg	btg
SiO2	76.46	75.79	73.69	73.13	73.39	74.14	75.60	74.64	74.58	74.91	73.21	71.23	72.74	73.41	69.90	74.74	76.22	74.99	71.62	69.50	72.30
TiO2	0.09	0.13	0.11	0.26	0.16	0.12	0.10	0.14	0.16	0.25	0.34	0.19	0.19	0.11	0.20	0.58	0.35	0.10	0.48	0.37	0.33
Al2O3	13.82	13.92	14.46	14.15	14.94	14.39	13.63	13.77	14.06	13.77	14.02	16.53	15.09	15.45	15.82	12.76	12.44	14.09	14.02	14.85	14.57
Fe2O3	0.93	0.96	1.10	1.76	1.70	1.32	1.45	0.81	1.08	1.37	1.83	1.56	1.85	1.03	1.21	3.07	1.85	0.76	2.53	1.95	1.91
MnO	0.04	0.07	0.09	0.05	0.05	0.06	0.07	0.06	0.03	0.04	0.07	0.05	0.07	0.06	0.11	0.14	0.05	0.06	0.06	0.04	0.05
MgO	0.05	0.22	0.10	0.51	0.31	0.24	0.20	0.14	0.24	0.33	0.67	0.48	0.23	0.23	0.38	1.24	0.50	0.16	0.71	0.55	0.49
CaO	0.38	0.45	0.46	0.92	0.82	0.53	0.50	0.36	0.46	0.56	2.02	0.90	0.82	0.64	0.85	2.53	0.81	0.44	1.24	0.96	0.79
Na2O	2.46	2.64	2.59	2.80	2.51	3.08	1.69	3.42	2.97	3.01	2.71	2.03	2.55	2.57	3.05	3.52	3.01	3.44	3.01	3.08	3.16
K2O	5.18	5.56	5.88	5.04	5.23	5.77	5.77	5.61	4.63	4.76	4.19	8.01	5.56	5.59	8.32	1.14	4.49	4.35	4.19	5.80	4.34
P2O5	0.14	0.11	0.15	0.12	0.24	0.17	0.15	0.26	0.27	0.30	0.04	0.17	0.32	0.13	0.03	0.20	0.28	0.36	0.35	0.35	0.27
LOI	0.45	0.15	1.63	1.26	0.65	0.18	0.84	0.72	0.85	1.00	0.90	0.04	0.58	0.78	0.13	0.08	0.05	1.01	0.92	0.98	1.31
Total	100.0	100.0	100.0	100.0	100.0	100.0	100.0	99.92	99.33	100.3	100.0	101.19	100.0	100.0	100.0	100.0	100.05	99.77	99.12	98.42	99.53

B	**SAUCE GUACHO GRANITE**										**SANTA ROSA GRANITE**										
Sample	6230	6231	6232	6233	6234	6237	6240	8000	8001	8006	6247	6250	6253	6254	6255	6463b	6467	8002	8003	8007	8027
Rock type	2m	2m	2m	2m	2m	2m	2m	2m	2m	2m	btg	btg	btg	btg	btg	btg	btg	btg	btg	mg	btg
Co	nd	nd	nd	nd	nd	nd	nd	13.00	18.00	17.00	nd	nd	nd	nd	nd	nd	nd	21.0	22.0	15.0	14.0
Sc	nd	nd	nd	nd	nd	nd	nd	3.00	5.00	3.00	nd	nd	nd	nd	nd	nd	nd	3.0	6.0	4.0	4.0
V	nd	nd	nd	nd	nd	nd	nd	13.00	17.00	23.00	nd	nd	nd	nd	nd	nd	nd	10.0	43.0	49.0	29.0
Pb	nd	nd	nd	nd	nd	nd	nd	42.00	15.00	24.00	nd	nd	nd	nd	nd	nd	nd	13.0	27.0	47.0	13.0
Zn	nd	nd	nd	nd	nd	nd	nd	60.00	40.00	60.00	nd	nd	nd	nd	nd	nd	nd	100.0	100.0	70.0	50.0
Rb	381.0	417.0	447.0	363.0	369.0	426.0	458.0	483.0	546.0	464.0	170.0	340.0	400.0	464.0	505.0	nd	nd	676.0	390.0	379.0	415.0
Cs	nd	nd	nd	nd	nd	nd	nd	19.0	20.3	21.9	nd	nd	nd	nd	nd	nd	nd	23.5	40.8	22.4	34.0
Ba	nd	nd	nd	nd	nd	nd	nd	80.0	64.0	248.0	nd	nd	nd	nd	nd	nd	nd	31.0	262.0	474.0	223.0
Sr	29.0	60.0	27.0	56.0	69.0	78.0	32.0	31.0	25.0	58.0	111.0	158.0	139.0	73.0	78.0	nd	nd	18.0	92.0	112.0	74.0
Tl	nd	nd	nd	nd	nd	nd	nd	2.9	2.9	2.7	nd	nd	nd	nd	nd	nd	nd	4.2	2.3	2.5	2.5
Ga	nd	nd	nd	nd	nd	nd	nd	22.0	29.0	25.0	nd	nd	nd	nd	nd	nd	nd	30.0	28.0	24.0	25.0
Li	101.0	100.0	101.0	115.0	100.0	92.0	88.0	nd	nd	nd	145.0	68.0	120.0	119.0	136.0	58.0	130.0	nd	nd	nd	nd
Ta	nd	nd	nd	nd	nd	nd	nd	5.3	5.3	5.4	nd	nd	nd	nd	nd	nd	nd	7.4	4.7	3.5	4.9
Nb	nd	nd	nd	nd	nd	nd	nd	23.0	33.0	27.0	nd	nd	nd	nd	nd	nd	nd	34.0	27.0	19.0	26.0
Hf	nd	nd	nd	nd	nd	nd	nd	1.4	1.9	3.9	nd	nd	nd	nd	nd	nd	nd	1.6	6.5	5.5	5.0
Zr	nd	nd	nd	nd	nd	nd	nd	57.0	66.0	137.0	nd	nd	nd	nd	nd	nd	nd	46.0	246.0	185.0	156.0
Y	nd	nd	nd	nd	nd	nd	nd	13.0	10.0	13.0	nd	nd	nd	nd	nd	nd	nd	9.0	25.0	19.0	23.0
Th	nd	nd	nd	nd	nd	nd	nd	7.3	12.7	26.7	nd	nd	nd	nd	nd	nd	nd	6.1	53.9	44.4	36.9
U	nd	nd	nd	nd	nd	nd	nd	2.7	3.0	4.8	nd	nd	nd	nd	nd	nd	nd	1.7	4.5	3.1	3.6
Be	6.1	4.5	6.3	9.4	9.2	6.6	5.0	5.0	6.0	20.0	38.0	7.9	7.4	12.0	16.0	3.2	16.4	4.0	16.0	8.0	11.0
La	nd	nd	nd	nd	nd	nd	nd	7.1	14.2	31.7	nd	nd	nd	nd	nd	nd	nd	9.2	68.6	57.8	52.8
Ce	nd	nd	nd	nd	nd	nd	nd	16.2	31.0	68.2	Nd	nd	nd	nd	nd	nd	nd	19.6	147.0	127.0	103.0
Pr	nd	nd	nd	nd	nd	nd	nd	1.95	3.76	8.49	nd	nd	nd	nd	nd	nd	nd	2.31	17.8	15.7	12.2
Nd	nd	nd	nd	nd	nd	nd	nd	7.4	13.8	31.0	nd	nd	nd	nd	nd	nd	nd	9.2	67.0	57.7	43.7
Sm	nd	nd	nd	nd	nd	nd	nd	1.6	2.9	6.1	nd	nd	nd	nd	nd	nd	nd	1.9	12.1	10.6	9.0
Eu	nd	nd	nd	nd	nd	nd	nd	0.21	0.25	0.56	nd	nd	nd	nd	nd	nd	nd	0.18	1.09	1.2	0.97
Gd	nd	nd	nd	nd	nd	nd	nd	1.4	2.0	4.0	nd	nd	nd	nd	nd	nd	nd	1.5	7.8	7.4	6.2
Tb	nd	nd	nd	nd	nd	nd	nd	0.3	0.3	0.6	nd	nd	nd	nd	nd	nd	nd	0.3	1.0	0.9	0.8
Dy	nd	nd	nd	nd	nd	nd	nd	1.7	1.7	2.6	nd	nd	nd	nd	nd	nd	nd	1.5	4.9	4.3	4.3
Ho	nd	nd	nd	nd	nd	nd	nd	0.3	0.3	0.4	nd	nd	nd	nd	nd	nd	nd	0.3	0.8	0.7	0.8
Er	nd	nd	nd	nd	nd	nd	nd	1.1	1.0	1.3	nd	nd	nd	nd	nd	nd	nd	0.9	2.5	2.1	2.5
Tm	nd	nd	nd	nd	nd	nd	nd	0.21	0.16	0.2	nd	nd	nd	nd	nd	nd	nd	0.16	0.38	0.3	0.37
Yb	nd	nd	nd	nd	nd	nd	nd	1.4	1.0	1.2	nd	nd	nd	nd	nd	nd	nd	1.0	2.3	1.8	2.3
Lu	nd	nd	nd	nd	nd	nd	nd	0.19	0.14	0.17	nd	nd	nd	nd	nd	nd	nd	0.13	0.31	0.26	0.33

2m = two mica granite; btg = biotite granite; mg = muscovite granite

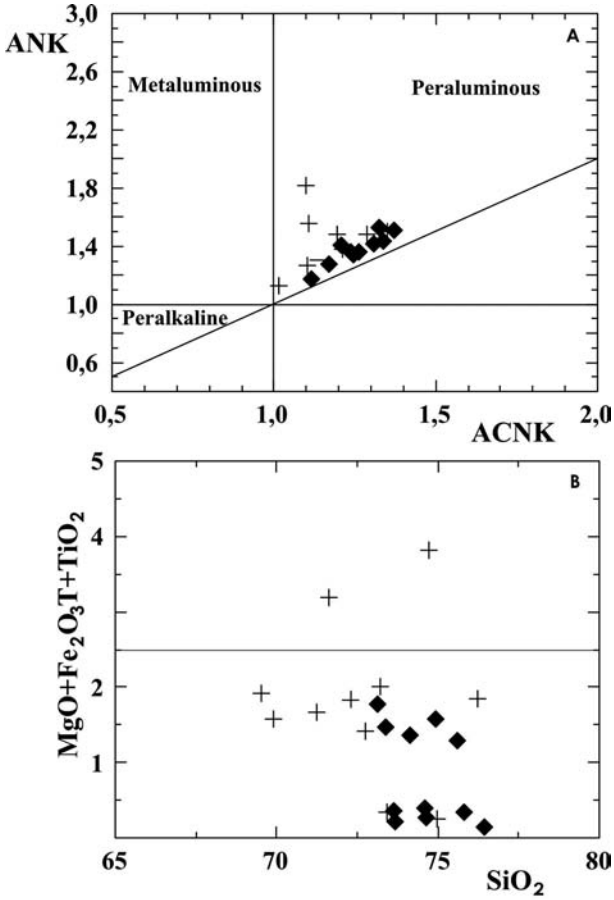

Fig. 2. **A**: ANK (Al_2O_3/[Na_2O+K_2O]) versus ACNK (Al_2O_3/[Na_2O+K_2O+CaO]) diagram. Santa Rosa granite (crosses) and Sauce Guacho granite (diamonds). **B**: MgO+FeOt+TiO_2 versus SiO_2 (wt%) showing values generally lower than 2.5, typical for the leucogranites.

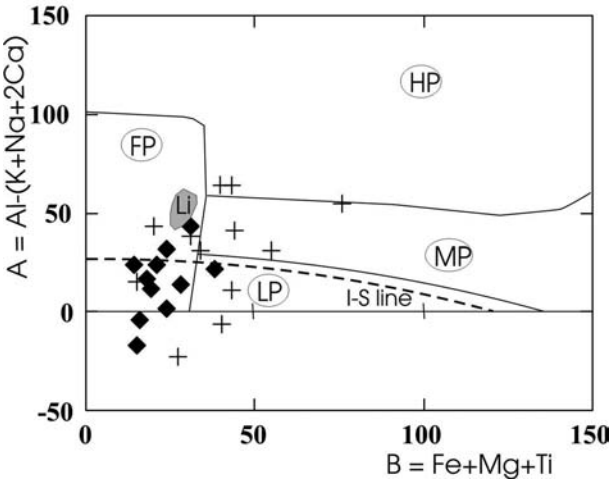

Fig. 4. A-B diagram after Villaseca et al. (1998) for distinguishing different granitic series. **HP =** highly peraluminous, **MP =** moderately peraluminous, **LP =** low peraluminous, **FP =** felsic peraluminous. **Dotted line =** I/S boundary. SG granite plots dominantly in the FP field, SR granite in different fields. **Li =** Limousin granite (Leger et al. 1990). Symbols as in Fig. 2.

teristic of leuco-granites (Fig. 2B). CIPW-normative calculation gives 37.42 vol% quartz, 31.91 vol% orthoclase, 23.54 vol% albite, 1.49 vol% anorthite and 3.21 vol% corundum. The normative corundum is characteristic of peraluminous granites.

The major oxides MgO, TiO_2, Fe_2O_{3t} versus SiO_2 show good correlation for the Sauce Guacho granite and some dispersion for the Santa Rosa granite. CaO, Al_2O_3, and MgO show some correlation versus SiO_2 (Fig. 3).

Villaseca et al. (1998) used the binary diagram of Debon & Le Fort (1983) along with a peraluminosity parameter (A = Al – [K + Na + 2Ca]) and a differentiation index B (= Fe + Mg + Ti) to suggest criteria for achieving a rigorous chemical-mineralogical definition. With this diagram it is possible to distinguish the four types of peraluminous granites that can be found in an orogenic segment. The SG and SR granites plot preferentially in the FP (felsic peraluminous) field (Fig. 4).

Trace elements

Contents of the trace elements Li and Be (67.4 ppm and 10.4 ppm respectively) are high in both granites suggesting that the granites have been the source of the spodumen- and beryl-rich pegmatites.

Figure 5 shows the diagram Rb versus Sr after Inger & Harris (1993). The samples of the SG granite plot in the field with a Rb/Sr ratio > 5, while Santa Rosa granite samples are found mostly in the field Rb/Sr < 5. In this diagram, Harris et al. (1993) and Inger & Harris (1993) assigned the upper field (Rb/Sr > 5) to a muscovite-rich source, and the lower field (Rb/Sr < 5) to a biotite-rich source.

In the tectonic discriminant diagram of Pearce et al. (1984), the studied samples plot in the field of syn-collision granites (Fig. 6) and are therefore in accordance with the muscovite-bearing peraluminous granitoid (MPG) type of Barbarin (1999).

Chondrite-normalized REE patterns are shown in Fig. 7. Generally, all the samples show a similar pat-

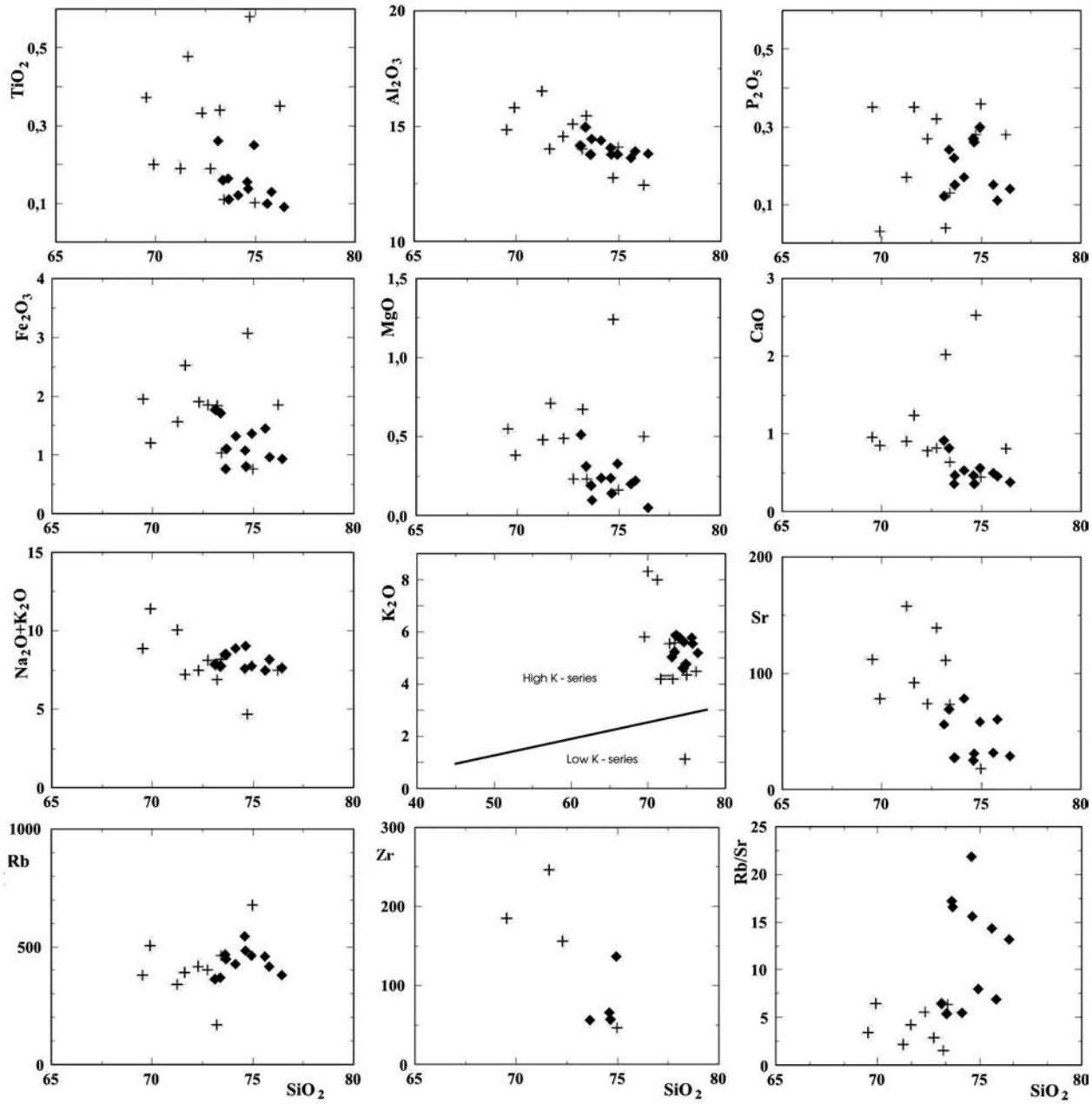

Fig. 3. Harker plots of selected major oxides and trace elements of the SR and SG granites. Symbols as in Fig. 2.

tern differing only in abundances with a slight LREE-enrichment. The Santa Rosa pluton displays a total REE content between 333.58 and 48.19 ppm, whereas the SG pluton has a total REE content between 156.52 and 40.87 ppm. All granites samples show moderate negative Eu anomalies with an Eu/Eu* mean value of 0.37 which suggests a feldspar fractionation in the source.

On a continental crust-normalized spidergram (Fig. 8) after Taylor & McLennan (1985), the samples exhibit strongly negative Ba, Sr and Ti anomalies and positive Rb, Th, K, Ta, Nd, Sm and Tb anomalies.

In the Q-Ab-Or diagram (Fig. 9), the two-mica leucogranites and muscovite-leucogranites plot close to the ternary minimum with Ptot = 100 MPa conditions (Johannes & Holtz 1996).

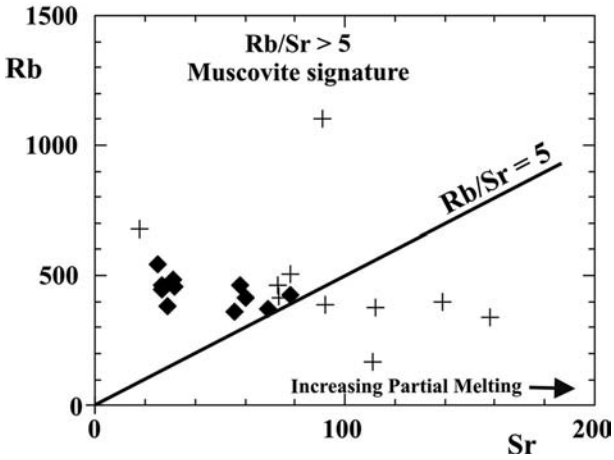

Fig. 5. Rb versus Sr diagram after INGER & HARRIS (1993). Symbols as in Fig. 2.

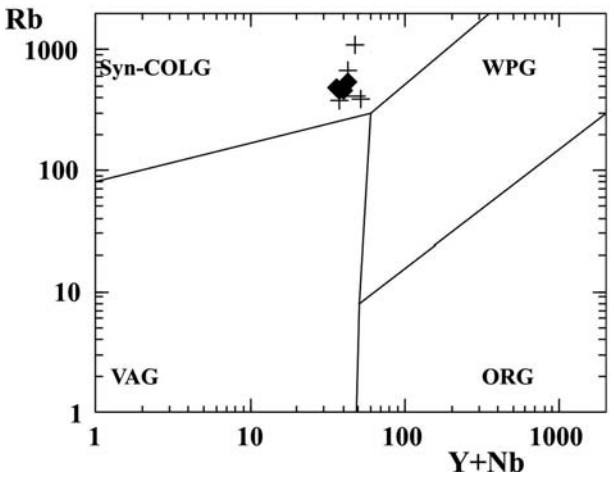

Fig. 6. Rb versus Y+Nb diagram after PEARCE et al. (1984). SG and SR granites plot in the Syn-COLG field. Symbols as in Fig. 2.

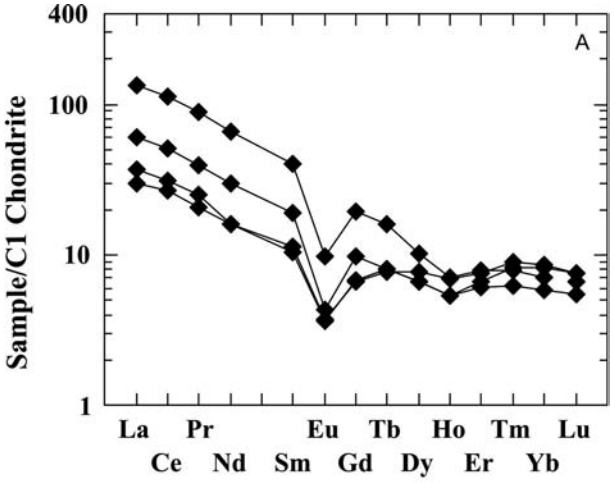

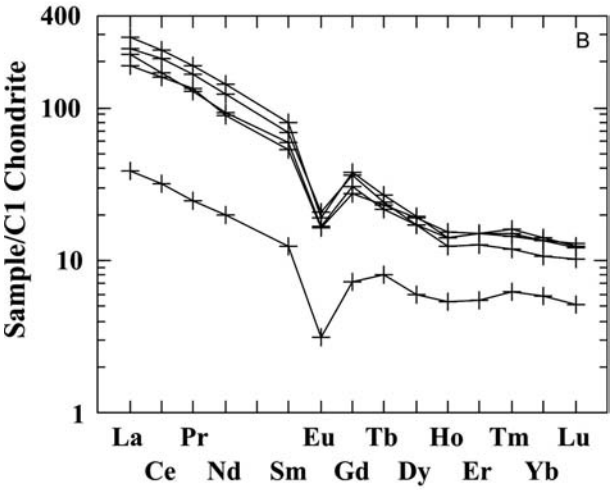

Fig. 7. Chondrite-normalized REE patterns. **A**: SG granite; **B**: SR granite and the fine grain leucogranite are REE-depleted. Note that all samples show negative Eu anomalies. Symbols as in Fig. 2.

U-Pb Geochronology

The zircon U-Pb IDTIMS analytical procedure at the Centro de Pesquisas Geocronológicas, IGc/USP, started with the sample being reduced to 100- and 250-mesh grain-sizes in a disc mill. The material was then classified in a Wilfley table and the portion rich in heavy minerals treated with bromoform and methyl iodide. The heavy concentrate was processed in a Frantz magnetic separator. Final purification was then carried out by hand-picking under the stereomicroscope. By adding HF and HNO_3 in Teflon microbombs with a $^{205}Pb/^{235}U$ spike, the zircon crystals were dissolved. U and Pb were concentrated and purified by passing the solution through an anionic exchange resin column. The solution enriched in U and Pb was deposited in a rhenium filament and the isotopic composition determined with a Finnigan MAT 262 solid source mass spectrometer. After reduction of the data (PBDAT), the results were plotted in appropriate diagrams using the software ISOPLOT/EX (LUDWIG 1998). The U-Pb data for both granites are given in the Table 2.

Table 2. Conventional zircon and monazite U-Pb analyses for the Santa Rosa granite.

SPU	Fraction	207/235#	Error [%]	206/238#	Error %	COEF.	238/206	Error [%]	207/206#	Error [%]	206/204*	Pb [ppm]	U [ppm]	Weight [µg]	206/238 Age [Ma]	207/235 Age [Ma]	207/206 Age [Ma]
3831	A MZ	0.37931	8.26	0.05915	3.19	0.392	16.90691	3.19	0.04651	7.60	134.46	315.1	309.7	1.82	370	327	324
3873	B ZR	0.30556	0.90	0.04210	0.72	0.818	23.75195	0.72	0.05264	0.52	136.2	14.0	211.7	23.19	266	271	313
3874	C ZR	0.48557	4.51	0.05585	4.35	0.968	17.90440	4.35	0.06305	1.14	229.3	12.1	207.5	26.11	350	402	710

SPU: Laboratory number; #: Radiogenic Pb corrected for blank and initial Pb; U corrected for blank
*Not corrected for blank or non-radiogenic Pb; Total U and Pb concentrations corrected for analytical blank
Ages: given in Ma using Ludwig Isoplot/Ex program (1998), decay constants recommended by Steiger & Jäger (1977)

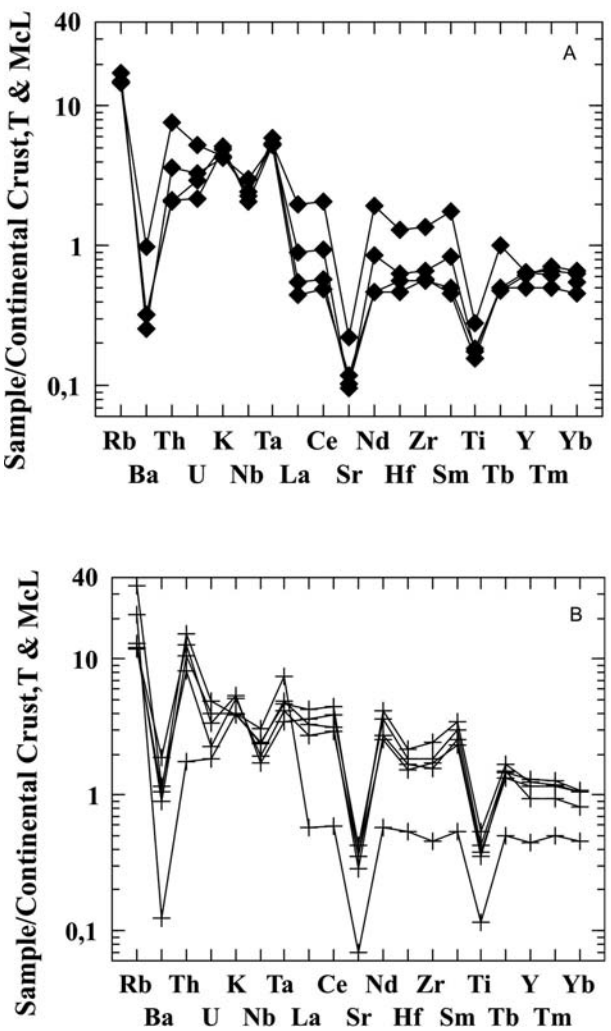

Fig. 8. Continental-crust normalized spidergram after Taylor & McLennan (1985). **A**: SG granite; **B**: SR granite. Note that all samples show negative Ba-, Sr- and Ti-anomalies and positive Rb, Th, Ta, Ce, Nd, Sm and Tb anomalies. Symbols as in Fig. 2.

The SR porphyritic granite (sample 8003) was dated by conventional U-Pb on zircon and monazite, the data are presented in a Tera-Wasserburg diagram (Fig. 10). In general, the analytical data indicate low values for the $^{206}Pb/^{204}Pb$ ratio. However, considered that the blank is 7 pg, these values possibly reflect the own characteristics of the dated granite minerals. In addition, the observed high degree of discordance and its scattered data in the diagram is a common feature from crustal melt peraluminous leucogranite zircons. The main reason for that is the inheritance of the zircons observable in these minerals and a recent Pb-loss. This characteristic is less common in monazites based on the reasons given above. The monazite fractions of the SR granite studied here yielded a $^{206}Pb/^{238}U$ mean age of 369.8 ± 5.3 Ma. This value it is not very different from the K-Ar age of 373 ± 10 Ma obtained in this pluton by Linares (1977).

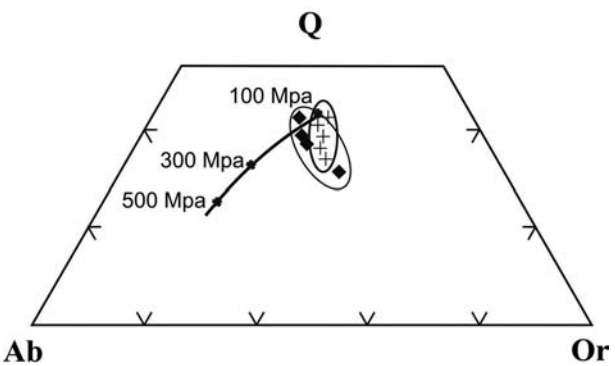

Fig. 9. Qtz-Ab-Or system at P_{tot} = 100-500 MPa and H_2O-saturated conditions (stars). Bold curve connect minimum (eutectic) melt compositions (Johannes & Holtz 1996). Symbols as in Fig. 2.

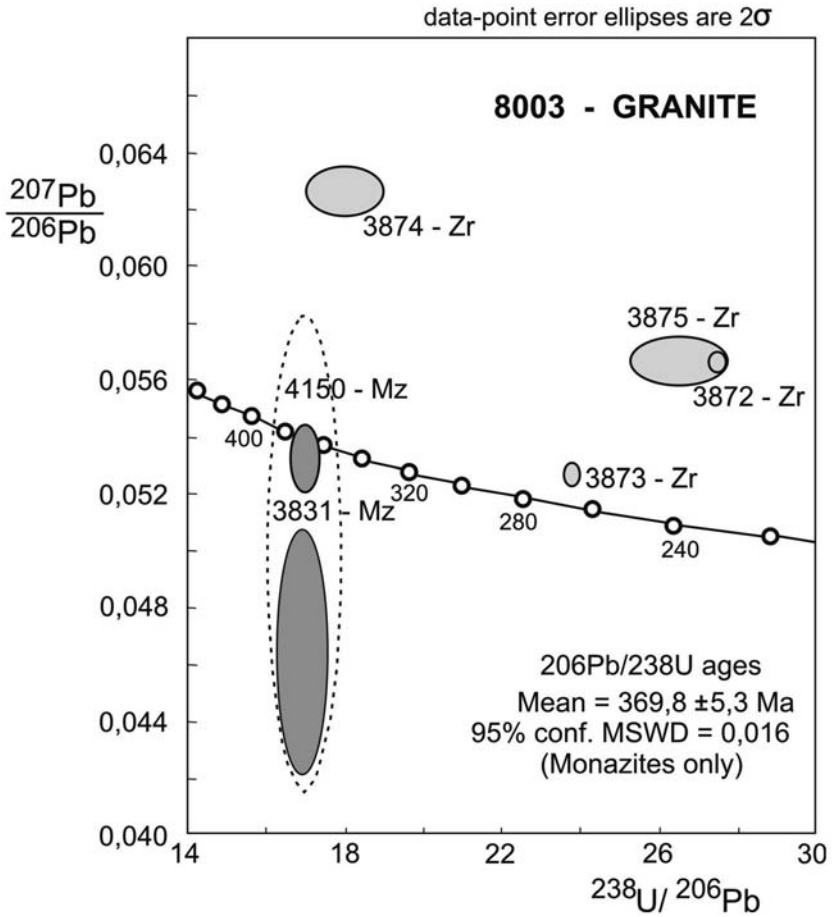

Fig. 10. Tera-Wasserburg Concordia diagram on axes of $^{207}Pb/^{206}Pb$ versus $^{238}U/^{206}Pb$ showing plot of zircon and monazite data for SR granite.

Sm – Nd isotope geochemistry

A Rb-Sr isochron for the SG granite obtained by Knüver (1983) yielded a high initial $^{87}Sr/^{86}Sr$ value of 0.716 and an age of 333.9 Ma, that is matched by a low $\varepsilon_{Nd(t)}$ of -5.3. Table 3 shows the Sm-Nd data for the SG and SR granites assessed in the present study.

The monazite U-Pb age (Table 2) has an uncertainty of only ± 5.3 Ma, so for this reason we assume an age of 370 Ma and $\varepsilon_{Nd(t)}$ of -5.3 for the SG granite and an age of 334 Ma and $\varepsilon_{Nd(t)}$ of -5.7 for the SR granite (Table 3).

The Sm-Nd crustal residence ages for the SG and SR granites are 1,544 and 1,571 Ma respectively, and were calculated using the multistage model of DePaolo et al. (1991). The model ages are in the same range as those of the Famatinian Arc granites (Lower Ordovician) in the Central Sierras Pampeanas (Pankhurst et al. 1998) and suggest a common Mesoproterozoic crustal provenance. These results are quite different from those obtained for the San Blas, Sanagasta, and Huaco Carboniferous porphyritic granites of the Sierra de Velasco, which have higher $\varepsilon_{Nd(t)}$ (-1.5 to -4.27) and younger model ages between 1,167 and 1,398 Ma (Grosse et al. 2009).

Discussion and interpretation

The SG and SR plutons are interpreted to be post-tectonic intrusions. Effects of contact metamorphism in the country rocks were not observed, probably because the emplacement of the plutons occurred on a hot country rocks environment with a limited development of contact zoning. Local miarolitic cavities indicate a shallow crustal intrusion.

Table 3. Sm-Nd data for the Sauce Guacho and Santa Rosa granites.

Sample	Sm [ppm]	Nd [ppm]	$^{147}Sm/^{144}Nd$	$^{143}Nd/^{144}Nd$	$(^{143}Nd/^{144}Nd)t$ 334 Ma	$\varepsilon_{Nd(t)}$	T_{DM} [Ma]
SG8001	2.9	13.8	0.1271	0.512197	0.511919	-5.6	1542
SR8003	12.1	67.0	0.1092	0.512132	0.511893	-6.1	1575

Constants: $^{147}Sm/^{144}Nd_{CHUR}$: 0.1967; $^{143}Nd/^{144}Nd_{CHUR}$: 0.512638; λ: 6.54 x 10^{-12}.

The SG and SR are leucogranites and contain < 5% mafic minerals, biotite and ilmenite, but not magnetite. CIPW-normative calculation determined a corundum content of 3.21 vol%, which is indicative of peraluminous granites.

The initial $^{87}Sr/^{86}Sr$ ratios of > 0.706 (SR) and > 0.7146 (SG) are characteristic of plutons that correspond to MPG-type (muscovite-peraluminous granite) after Barbarin (1999), anatectic leucogranites (Lameyre 1988), hercynotype-oblique continental collision with regional low-pressure metamorphism (Pitcher 1982), and/or highly FP (felsic peraluminous) granitoids (Villaseca et al. 1998).

The high values of the Rb/Sr ratio (> 9) in the SG granite suggest that these leucogranites derived by muscovite dehydration melting (Inger & Harris 1993; Harris et al. 1993). Conversely, the lower Rb/Sr ratios (< 4) suggest the participation of biotite during melt production, as indicated also by the petrographic and geochemical features. These are reasonable sources, which explains the high content of Li and Be as well as of K, Rb and Cs, which are concentrated in biotite and muscovite (London 2008).

The genesis of peraluminous granitoids is not only controlled by the nature of the sources, but mainly by the conditions of crustal anatexis. The MPG granites are formed where the anatexis of crust is affected by major shears or thrusts.

Peraluminous MPG are mainly emplaced where crustal thickening results from the convergence of two continental lithospheres and are concentrated along the transcurrent shear and thrust zones that crosscut the thick crust (Barbarin 1996, 1999). In high temperature collision belts, the crust remains comparatively thin (< 50 km) and hot (> 875 ºC) (Sylvester 1998), and the peraluminous granite magmatism is primarily the product of a post-collisional, mantle-derived heat source.

There is no applicable mineral barometer to determine the emplacement depth of these granites. However, an indication for the emplacement depth is provided by the CIPW-normative Qz-Ab-Or diagram, where most samples plot in the low temperature field near 5 kb, and to the right of the cotectic/eutectic minima of the H_2O-saturated haplogranite system, which is typical of high-level emplacement of natural low-temperature granites (Johannes & Holtz 1996).

Experimental results confirm that two-mica granites crystallize under high water-fugacity conditions. The initial water content in the melt must have amounted to about 7 to 8% to allow muscovite to precipitate (Wyllie 1977). This water can be provided by major thrust or shear zones that concentrate and channel fluids in the crust during collision-convergent tectonics (Strong & Hammer 1981). These fluids promoted extensive melting and, moreover, lubricated the shear zones controlling the elongation of the plutons that lies parallel to the tectonic structure.

The MPG is associated with the climax of orogenesis. The magmas formed during the compressive tectonics and were not emplaced until there was tension either along some shear zones (transtension) or during local relaxation. The composition of leucogranites suggests that the magma was generated by partial melting of Ancasti Formation schists.

The intrusive MPG represents the upper emplacement levels. Therefore, the SG and SR stocks which are emplaced within regional shear zones would belong to this granite type.

These granitoids are practically free of opaque oxides, and may have originated at a medium crust pressure, under conditions of low oxygen fugacity similar to those of ilmenite-series granitoids (Ishihara 1977), with very low magnetic susceptibility. In both leucogranite types, the high contents of alkaline elements, such as K, Rb and Cs, are the signature of biotite and muscovite breakdown (Icenhower & London 1996). However, of the two phyllosilicates, only biotite can enrich the melt with Ti (SR, average 1745 ppm; SG, average 906 ppm), demonstrating that only in their production were significant amounts of biotite involved.

Prograde metamorphism of muscovite-rich and biotite-rich metapelite sources may have produced both types of leucogranites found in the study area: in SG by dehydration melting in muscovite-rich (Mu > Bt), in SR by dehydration melting in biotite-rich metapelites (Bt > Mu).

Although the leucogranites of SG and SR intruded in host rocks at high crustal level (as indicated by muscovite and biotite) these minerals crystallized from the melt. The solidus temperature may have been lowered by considerable quantities of B (tourmaline) and F (fluorite) in the melt (Manning 1981; Pichavant 1987) so that muscovite crystallized from the melt at a pressure < 4 kb. Hence, both production and emplacement of SR and SG magmas occurred inside the upper crust, and magma ascent was limited, as is the case in nearly H_2O-saturated melts produced by fluid-excess melting (Clemens & Droop 1998).

Sm-Nd isotope data indicate an $\varepsilon_{Nd(t)}$ of -5.3 for the SG granite and an $\varepsilon_{Nd(t)}$ of -5.7 for the SR granite which suggests a crustal provenance. The model Nd ages of 1,544 Ma (SG) and 1,571 Ma (SR) are in the same range as those of the Famatinian Arc in the Central Sierras Pampeanas (Lower Ordovician) granites indicating that they have a common Mesoproterozoic source, probably the Puncoviscana Formation or metamorphic equivalents (Bock et al. 2000). In contrast, the Carboniferous San Blas, Huaco and Sanagasta granites (Sierra de Velasco) have εNd(t) values between -4.3 and -1.4, and younger times (Upper Mesoproterozoic) of crustal residence that suggest some participation of a more primitive mantle-derived component (Grosse et al. 2009)

Conclusions

The peraluminous leucogranite plutons, Santa Rosa (SR) and Sauce Guacho (SG), are interpreted to be typical products of partial melting of the continental crust that have formed at medium crust pressures as a result of post-collisional tectonic-setting. The Tera-Wasserburg Concordia diagram defined a $^{206}Pb/^{238}U$ value of 369.8 ± 5.3 Ma for the SR granite, and the Rb/Sr isochron gave a value of 333.9 ± 10.7 Ma for SG granite. The Nd isotopes present an $\varepsilon_{Nd(t)}$ of -5.3 for SG and an $\varepsilon_{Nd(t)}$ of -5.7 for the SR granites indicating their crustal provenance, without detectable mantle contribution. The model ages of 1,544 and 1,571 Ma are similar to those of the Famatinian Arc in the Central Sierras Pampeanas.

Mineralogical and geochemical compositions of SR and SG are typical of MPGs (muscovite peraluminous granites). The genesis of the plutons is suggested to have been related to shear zones in the metasedimentary crust (Ancasti Formation schists) during transpressive collision that promoted extensive melting.

The pegmatites cross-cutting both plutons and showing beryl, tourmaline and spodumen, and fluorite veins are related to the SR and SG plutons with both pegmatites and plutons being fertile granites rich in Be, B, F and Li elements.

Radial fractures are developed outside of the pluton and evidence the shallow intrusion of the plutons that lifted the metamorphic dome. Besides, porphyritic textures and miarolitic cavities indicate a shallow level of intrusion.

Acknowledgements

The authors are grateful to the Universidad Nacional de Tucumán for supporting project CIUNT - 26G438, to CONICET for supporting Project PIP Nº 0595, and to the Instituto de Geociencias of the Universidad de São Paulo for its general support. Valuable recommendations for improving the manuscript by Prof. Dr. Antonio Castro Dorado, Huelva, and by an anonymous reviewer are thankfully acknowledged.

References

Arrospide, A. (1985): Las manifestaciones de greisen de la Sierra de Fiambalá, Catamarca. – Revista de la Asociación Geológica Argentina, **40**: 97-113.

Barbarin, B. (1996): Genesis of the two main types of peraluminous granitoids. – Geology, **24** (4): 295-298.

Barbarin, B. (1999): A review of the relationships between granitoid types, their origin and their geodynamic environments. – Lithos, **46**: 605-626.

Bock, B., Bahlburg, H., Wörner, G. & Zimmerman, U. (2000): Tracing crustal evolution in the Southern Central Andes from Late Precambrian to Permian with geochemical and Nd and Pb isotope data. – Journal of Geology, **108**: 515-535.

Clemens, J. & Droop, G. (1998): Fluids, P-T paths and the fates of anatectic melts in the Earth´s crust. – Lithos, **44**: 21-36.

Debon, F. & Le Fort, P. (1983): A chemical-mineralogical classification of common plutonic rocks and associations. – Transactions of the Royal Society of Edinburgh: Earth Sciences, **73**: 135-149.

DePaolo, D.J., Linn, A.M. & Schubert, G. (1991) The crustal age distribution; methods of determining mantle separation ages from Sm-Nd isotopic data and application to the Southwestern United States. – Journal of Geophysical Research, **B96**: 2071-2088.

Grissom, G.C., DeBari, S.M. & Snee, L. (1998): Geology of the Sierra de Fiambalá, northwest Argentina: implications for early Paleozoic Andean Tectonics. – In: Pankhurst, R.J. & Rapela, C.W. (Eds.): The Proto-Andean margin of Gondwana. – Geological Society Special Publication, **142**: 297-323.

Grosse, P., Söllner, F., Báez, M.A., Toselli, A.J., Rossi, J.N. & De al Rosa, J.D. (2009): Lower Carboniferous post-orogenic granites in Central Eastern Sierra de Velasco, Sierras Pampeanas, Argentina: U-Pb monazite geochronology, geochemistry and Sr-Nd isotopes. – International Journal of Earth Sciences, **98**: 1001-1025.

Harris, N., Inger, S. & Massey, J. (1993) The role of fluids in the formation of High Himalayan leucogranites. – In: Treloar, P.J. & Searle, M.P. (Eds.): Himalayan Tectonics. – Geological Society of America, Special Papers, **74**: 391-400.

Icenhower, J. & London, D. (1996): Experimental partitioning of Rb, Cs, Sr, and Ba between alkali feldspar and peraluminous melt. – The American Mineralogist, **81**: 719-734.

Inger, S. & Harris, N. (1993) Geochemical constraints on leucogranite magmatism in the Lantang valley, Nepal Himalaya. – Journal of Petrology, **34**: 345-368.

Ishihara, S. (1977): The magnetite-series and ilmenite-series granitic rocks. – Mining Geology, **27**: 293-305.

Ishihara, S. (1981): The granitoid series and mineralization. – Economic Geology, 75th anniversary volume: 458-484.

Johannes, W. & Holtz, F. (1996): Petrogenesis and experimental petrology of granitic rocks. – Minerals and Rocks, **22:** 335 pp.

Knüver, M. (1983): Dataciones radimétricas de rocas plutónicos y metamórficas. – In: Aceñolaza, F.G., Miller, H. & Toselli, A.J. (Eds.): Geología de la Sierra de Ancasti. – Münstersche Forschungen zur Geologie und Paläontologie, **59**: 201-218.

Knüver, M. & Miller, H. (1982): Rb-Sr geochronology of the Sierra de Ancasti (Pampean Ranges, NW-Argentina). – Actas Vº Congreso Latinoamericano de Geología Buenos Aires, **3**: 457-471.

Manning, D. (1981): The effect of the fluorine on liquids phase relationships in the system Qz-Ab-Or with excess water at 1 kbar. – Contributions to Mineralogy and Petrology, **76**: 206-215.

Lameyre, J. (1988): Granite settings and tectonics. – Rendiconti della Societá Italiana di Mineralogía e Petrología, **43**: 215-236.

Lazarte, J.E., Avila, J.C., Fogliatta, A.S. & Gianfrancisco, M. (2006): Granitos evolucionados relacionados a mineralización estanno-wolframífera en Sierras Pampeanas Occidentales. – Serie Correlación Geológica, **21**: 75-104.

Lazarte, J.E.,Fernández Turiel, J.L., Guido, F. & Medina, M. (1999): Los granitos Río Rodeo y Quimivil: dos etapas del magmatismo paleozoico de Sierras Pampeanas. – Revista de la Asociación Geológica Argentina, **54** (4): 333-352.

Leger, J.M., Wang, X. & Lameyre, J. (1990): Les leucogranites de Saint-Goussaud en Limousin: pétrographie, éléments majeurs et traces dans le sondage de Villechabrolle. – Bulletin de la Société géologique de la France, **VI**: 515-524.

Linares, E. (1977): Catálogo de edades radiométricas determinadas para la República Argentina II: Años 1974-1976 y edades radimétricas realizadas por el INGEIS y sin publicar: Años 1972-1974. – Publicación Especial de la Asociación Geológica Argentina, **B** (4): 38 pp.

London, D. (2008): Pegmatites. – The Canadian Mineralogist, Special Publication, **10**: 347 pp.

Ludwig, K.R. (1998): Using Isoplot/Ex. – a geochronological toolkit for Microsoft Excel. – Berkeley Geochronology Center, Special Publication, **1** (Berkeley, USA).

Manning, D. (1981): The effect of the fluorine on liquids phase relationships in the system QZ-Ab-Or with excess water at 1 kbar. – Contributions to Mineralogy and Petrology, **76**: 206-215.

Neugebauer, H. (1995): Die Mylonite von Fiambalá – strukturgeologische und petrographische Untersuchungen an der Ostgrenze des Famatina-Systems, Sierra de Fiambalá, NW-Argentinien. – 109 pp.; unpublished doctoral thesis (Munich University).

Pankhurst, R.J., Rapela, C.W., Saavedra, J., Baldo, E., Dahlquist, J., Pascua, I. & Fanning, C.M. (1998): The Famatinian magmatic arc in the central Sierras Pampeanas: an Early to Mid-Ordovician continental arc on the Gondwana margin. – In: Pankhurst, R.J. & Rapela, C.W. (Eds.): The Protoandean margin of Gondwana. – Geological Society, London, Special Publications, **142**: 343-367.

Pearce, J.A., Harris, N.B.W. & Tindle, A.G. (1984): Trace element discrimination diagrams for the tectonic interpretation of granitic rocks. – Journal of Petrology, **25** (4): 956-983.

Pichavant, M. (1987): Effects of B and H2O on liquid phase relations in the haplogranitic system at 1 kbar. – The American Mineralogist, **72**: 1056-1070.

Pitcher, W.S. (1982): Granite type and tectonic environment. – In: Hsü, K. (Ed.): Mountain building processes. – Academic Press: 19-40.

Reissinger, M. (1983): Evolución geoquímica de las rocas plutónicas. – In: Aceñolaza, F.G., Miller, H. & Toselli, A.J. (Eds.): Geología de la Sierra de Ancasti. – Münstersche Forschungen zur Geologie und Paläontologie, **59**: 101-112.

Reissinger, M. & Miller, H. (1982): Geochemical evolution of Paleozoic plutonites in the Sierra de Ancasti (NW Argentina). – Actas Vº Congreso Latinoamericano de Geología Buenos Aires, **3**: 473-486.

Söllner, F., Gerdes, A., Grosse, P. & Toselli, A.J. (2007): U-Pb age determinations by LA-ICP-MS on zircons of the Huaco granite, Sierra de Velasco (NW-Argentina): A long-term history of melt activity within an igneous body. – Abstracts 20th Colloquium on Latin American Earth Sciences Kiel: 57.

Steiger, R.H. & Jäger, E. (1977): Subcommission on geochronology: convention on the use of decay constants in geochronology and cosmochronology. – Earth and Planetary Science Letters, **36:** 359-362.

Strong, D.F. & Hammer, S.K. (1981): The leucogranites of southern Brittany: Origin by faulting, frictional heating, fluid flux and fractional melting. – The Canadian Mineralogist, **19**: 163-176.

Sylvester, P.J. (1998): Post-collisional strongly peraluminous granites. – Lithos, **45**: 29-44.

Taylor, R.S. & McLennan, S. (1985): The continental crust: its composition and evolution. – 312 pp.; Oxford (Blackwell).

Toselli, A.J., Miller, H., Aceñolaza, F.G., Rossi, J.N. & Söllner, F. (2007): The Sierra de Velasco (northwestern Argentina) – an example for polyphase magmatism at the margin of Gondwana. – Neues Jahrbuch für Geologie und Paläontologie, Abhandlungen, **246** (3): 325-345.

Toselli, A.J., Reissinger, M. & Durand, F.R. (1983): Rocas graníticas. – In: Aceñolaza, F.G., Miller, H. & Toselli, A.J. (Eds.): Geología de la Sierra de Ancasti. – Münstersche Forschungen zur Geologie und Paläontologie, **59**: 79-100.

Toselli, A.J., Rossi, J.N., Báez, M.A., Grosse, P. & Sardi, F. (2006): El batolito Carbonífero Aimogasta, Sierra de Velasco, La Rioja, Argentina. – Serie Correlación Geológica, **21** (2): 137-154.

Toselli, A.J., Sial, A.N. & Rossi, J.N. (2002): Ordovician magmatism of the Sierras Pampeanas, Sistema de Famatina and Cordillera Oriental, NW of Argentina. – In: Aceñolaza, F.G. (Ed.): Aspects of the Ordovician System in Argentina. – Serie Correlación Geológica, **16**: 313-326.

Villaseca, C., Barbero, L. & Herreros, V. (1998): A reexamination of the typology of peraluminous granite types in intracontinental orogenic belts. – Transactions of the Royal Society of Edinburgh: Earth Sciences, **89**: 113-119.

Willner, A.P. (1983): Evolución Metamórfica. – In: Aceñolaza, F.G., Miller, H. & Toselli, A.J. (Eds.): Geología de la Sierra de Ancasti. – Münstersche Forschungen zur Geologie und Paläontologie, **59**: 189-200.

Wyllie, P.J. (1977): Crustal anatexis: an experimental review. – Tectonophysics **43**: 41-71.

Manuscript received: October 28, 2009.
Revised version accepted by the Munich editor: August 9, 2010.

Addresses of the authors:

Alejandro J. Toselli, Juana N. Rossi, Instituto Superior de Correlación Geológica (INSUGEO), Miguel Lillo 205, 4000 San Miguel de Tucumán, Argentina.
E-mail: ajtoselli@yahoo.com.ar

Miguel A.S. Basei, Claudia R. Passarelli, Instituto de Geociencias, Universidade de São Paulo, Rua do Lago 562, São Paulo, Brazil. E-mail: baseimas@spider.usp.br